PERGAMON

International Journal of Solids and Structures 39 (2002) 1817–1831

INTERNATIONAL JOURNAL OF SOLIDS and STRUCTURES

www.elsevier.com/locate/ijsolstr

Effect of porosity on the properties of strain localization in porous media under undrained conditions

Yong-Qiang Zhang [a,*], Hong Hao [a], Mao-Hong Yu [b]

[a] *Protective Technology Research Center, School of Civil and Structural Engineering, Nanyang Technological University, Singapore 639798, Singapore*

[b] *School of Civil Engineering and Mechanics, Xi'an Jiaotong University, Xi'an 710049, China*

Received 20 June 2001; received in revised form 6 November 2001

Abstract

Within the general framework of mixture theory and by introducing the fictitious "fluid phase" as a mixture of a liquid and a gas, the conditions for localization of deformation into a shear band in the incremental response of partially saturated and fully saturated elastic–plastic porous media under undrained conditions are derived. The effect of porosity is included in the derivation. The explicit analytical expressions of the direction of shear band initiation and the corresponding hardening modulus of the porous media for the plane strain case are deduced, and a parametric analysis is made of the influence of the porosity on the properties of strain localization based on Mohr–Coulomb yield criterion. It is found that the dependence of the shear banding properties of partially saturated porous media on the porosity is related to the stress states and Poisson's ratio. However, the properties of the strain localization for the fully saturated porous media are almost independent of Poisson's ratio. Finally, on the basis of Mohr–Coulomb yield criterion, some solutions of the shear banding orientation for water-saturated granular materials are obtained, which are proved to be in good agreement with the experimental results reported by other researchers.

Keywords: Porosity; Strain localization; Porous medium; Undrained condition

1. Introduction

Strain localization of plastic flow into shear bands is observed on a wide class of engineering materials, including metals, soils, concretes and rocks. Localized deformation is typically followed by a reduction in overall strength of the material body as loading proceeds (Read and Hegemier, 1984). It is therefore of considerable interest as a precursor of failure phenomena. A suitable tool for describing localization in solid mechanics is based on the strain rate discontinuity in continuum theory. It was first proposed by Hadamard (1903) and later developed by Thomas (1961), Hill (1962), Mandel (1963), and Rice (1976). It was applied to predict the existence and orientation of shear bands within various types of materials (Rudnicki and

* Corresponding author.
E-mail address: cyqzhang@ntu.edu.sg (Y.-Q. Zhang).

PII: S0020-7683(02)00010-0

Rice, 1975; Rice and Rudnicki, 1980; Vardoulakis, 1980; Molenkamp, 1985; Ottosen and Runesson, 1991; Runesson et al., 1991; Bigoni and Hueckel, 1991a,b; Schreyer and Zhou, 1995; Życzkowski, 1999).

Most of the works published so far only involve the behavior of single-phase materials. However, strain localization phenomena are also relevant for elastic–plastic porous solids. Strain localization for this sort of materials is generally discussed under locally undrained conditions. Some results can be found from the papers by Rice (1975), Rice and Cleary (1976), Rudnicki (1983) and Han and Vardoulakis (1991). The effect of pore fluid compressibility on localization in elastic–plastic porous solids subjected to undrained conditions was investigated by Runesson et al. (1996). Zhang and Schrefler (2001) studied the conditions for localization of deformation into a planar (shear) band and loss of uniqueness in the incremental response of elastic–plastic saturated porous media.

For porous media, porosity is an important material parameter. Therefore in this paper, based on the theory of mixtures (Bowen, 1982), the porosity is taken into account in the analysis of strain localization of partially saturated and fully saturated porous media under undrained conditions. The porous body is assumed to be elastic–plastic, subjected to small deformations and obeying a quite general non-associated flow rule. It is revealed from the investigation that the influence of the porosity on the onset of strain localization is of great significance. The result is in good agreement with the experiment data obtained by Han and Vardoulakis (1991).

Notations and conventions: Compact or index tensorial notation will be used throughout the paper. Tensor quantities are identified by boldface letters. Symbols '.' and ':' between tensors of various orders denote their inner product with single and double contraction, respectively. The dyadic product of two tensors is indicated with '$\otimes$'. $\boldsymbol{\delta}$ denotes the second-order identity tensor (Kronecker delta). $\mathbf{I}$ denotes the fourth-order identity tensor, which is defined as $I_{ijkl} = (1/2)(\delta_{ik}\delta_{jl} + \delta_{il}\delta_{jk})$. Summation applies over repeated mute Latin indices but, unless otherwise stated, not over Greek indices. 'tr' denotes the trace operator, e.g. for the second-order symmetric stress tensor $\boldsymbol{\sigma}$, $\mathrm{tr}\,\boldsymbol{\sigma} = \sigma_{ii}$.

2. Elastic–plastic constitutive equations for porous media under undrained conditions

The theory of mixtures is an effective method to deal with multiphase porous media such as soils and fissured rocks (Bowen, 1982). In practical engineering, the porous media are generally three-phase systems which consist of solid phase, liquid phase and gas phase. Fully saturated porous media are only made up of two constituents, a solid and a liquid. Therefore, whether the gas phase exists in the porous solid or not is the symbol to differentiate the partially saturated and fully saturated porous media. Both the liquid phase and the gas phase should be described accurately in order to effectively expound the properties of deformations and strengths of the media. The liquid phase usually can be described by Navier–Stokes equation and the gas phase by the gas equation of state (Zienkiewicz et al., 1993). However, the gas phase of the porous body in practical engineering is usually the mixture of vapor and air. In general, only dry air can be accurately described by the equation of state of idealized gas. It is difficult to delineate the state of the mixed gas due to the existence of vapor. For this reason, a fictitious "fluid phase" is assumed to simulate the mixture that consists of the actual liquid phase and gas phase, whose property is determined by those of the actual liquid phase and gas phase. It is feasible as the actual liquid phase has some dissolved air and is a mixture of liquid and gas, whereas the actual gas phase can be considered as the mixture made up of the undissolved air and vapor.

The degree of saturation of porous media can be modeled by the compressibility of the "fluid phase". A liquid can usually be thought of having little compressibility. However, an actual gas has much compressibility. Consequently, the "fluid phase" should have some degree of compressibility as a mixture of a liquid and a gas, and the compressibility increases with the increment of the gas content. Thus it can reflect the degree of unsaturation of the porous media indirectly with the compressible "fluid phase" model.

Thus, the porous media in geotechnical engineering can be modeled as mixtures made up of solid phase (S) and “fluid phase” (F), and the “fluid phase” consists of liquid (L) and undissolved gas (G). Each phase has a mass M_α and a volume V_α, $\alpha = \mathrm{S}$, F, which make up the total mass $M = M_\mathrm{S} + M_\mathrm{F}$ and the total volume $V = V_\mathrm{S} + V_\mathrm{F}$.

The intrinsic quantities, labeled by superscript R, and the apparent or partial quantities are defined at each point of each phase. For example, the intrinsic mass density is defined as $\rho_\alpha^\mathrm{R} = M_\alpha / V_\alpha$, whereas the apparent mass density is defined by $\rho_\alpha = M_\alpha / V$. Hence, $\rho_\alpha = m_\alpha \rho_\alpha^\mathrm{R}$, where $m_\alpha = V_\alpha / V$ is the volume fraction of phase α. For the porous media in geotechnical engineering, it has

$$m_\mathrm{S} + m_\mathrm{F} = 1 \tag{1}$$

where the volume fraction m_F of “fluid phase” is just the porosity of the porous body.

If the contribution due to diffusion is ignored, the total stress tensor of the mixture is

$$\boldsymbol{\sigma} = \boldsymbol{\sigma}_\mathrm{S} + \boldsymbol{\sigma}_\mathrm{F} = (1 - m_\mathrm{F})\boldsymbol{\sigma}_\mathrm{S}^\mathrm{R} + m_\mathrm{F}\boldsymbol{\sigma}_\mathrm{F}^\mathrm{R} \tag{2}$$

and the strain rate tensor of each phase has (Yang and Yu, 2000)

$$\dot{\boldsymbol{\varepsilon}}_\alpha = \dot{\boldsymbol{\varepsilon}}, \quad \alpha = \mathrm{S}, \mathrm{F} \tag{3}$$

In Eq. (2), $\boldsymbol{\sigma}_\alpha$ is the partial stress tensor and $\boldsymbol{\sigma}_\alpha^\mathrm{R}$ the intrinsic stress tensor, $\alpha = \mathrm{S}$, F. If the internal structure remains constant during the deformation process, namely m_α, $\alpha = \mathrm{S}$, F will not change, it has

$$\dot{\boldsymbol{\sigma}} = \dot{\boldsymbol{\sigma}}_\mathrm{S} + \dot{\boldsymbol{\sigma}}_\mathrm{F} = (1 - m_\mathrm{F})\dot{\boldsymbol{\sigma}}_\mathrm{S}^\mathrm{R} + m_\mathrm{F}\dot{\boldsymbol{\sigma}}_\mathrm{F}^\mathrm{R} \tag{4}$$

If the internal structure of the “fluid phase” as a two-phase mixture remains the same, i.e., no phase transition happens, and the “fluid phase” follows the elasticity laws, it has

$$\dot{\boldsymbol{\sigma}}_\mathrm{F}^\mathrm{R} = \dot{P}_\mathrm{F}^\mathrm{R}\boldsymbol{\delta} = K_\mathrm{F}(\boldsymbol{\delta} \otimes \boldsymbol{\delta}) : \dot{\boldsymbol{\varepsilon}} \tag{5}$$

under undrained conditions, where compression is defined as positive, P_F^R is the intrinsic pore pressure,

$$\dot{P}_\mathrm{F}^\mathrm{R} = K_\mathrm{F}(\boldsymbol{\delta} : \dot{\boldsymbol{\varepsilon}}) \tag{6}$$

and K_F is the bulk compression modulus of the “fluid phase”, which is defined as follows:

$$K_\mathrm{F} = m_\mathrm{L}K_\mathrm{L} + (1 - m_\mathrm{L})K_\mathrm{G} \tag{7}$$

where K_L and K_G are the bulk modulus of the liquid and gas, respectively; m_L is the volume fraction of the liquid in the “fluid phase”, namely the so-called degree of saturation in soil mechanics, which is defined by the equation $m_\mathrm{L} = V_\mathrm{L}/V_\mathrm{F}$.

It is well known that the deformation and strength of porous media (e.g. soils) under loading is not determined directly by the total stress but the effective stress, which can be defined as (Terzaghi, 1943)

$$\boldsymbol{\sigma}' = \boldsymbol{\sigma} - \boldsymbol{\sigma}_\mathrm{F}^\mathrm{R} \tag{8}$$

From Eq. (8), we have

$$\dot{\boldsymbol{\sigma}}' = \dot{\boldsymbol{\sigma}} - \dot{\boldsymbol{\sigma}}_\mathrm{F}^\mathrm{R} \tag{9}$$

Substituting Eq. (4) into Eq. (9), we obtain

$$\dot{\boldsymbol{\sigma}}' = (1 - m_\mathrm{F})(\dot{\boldsymbol{\sigma}}_\mathrm{S}^\mathrm{R} - \dot{\boldsymbol{\sigma}}_\mathrm{F}^\mathrm{R}) \tag{10}$$

Defining the yield function F and the plastic potential G in the effective stress space, the relation between the effective stress and strain can be expressed as

$$\dot{\boldsymbol{\sigma}}' = \mathbf{E}' : \dot{\boldsymbol{\varepsilon}} \quad \text{elastic unloading} \tag{11}$$

$$\dot{\boldsymbol{\sigma}}' = \mathbf{D}' : \dot{\boldsymbol{\varepsilon}} \quad \text{plastic loading} \tag{12}$$

where the effective elastic tangent stiffness tensor $\mathbf{E}'$ is defined as

$$\mathbf{E}' = (1 - m_F)(\mathbf{E}_S - K_F(\boldsymbol{\delta} \otimes \boldsymbol{\delta})) \tag{13}$$

in which $\mathbf{E}_S$ is the elastic tangent stiffness tensor of the solid phase in the porous body, and the effective elastic–plastic tangent stiffness tensor $\mathbf{D}'$ is given as

$$\mathbf{D}' = \mathbf{E}' - \frac{1}{A'}(\mathbf{E}' : \mathbf{Q}') \otimes (\mathbf{P}' : \mathbf{E}') \tag{14}$$

where

$$\mathbf{P}' = \frac{\partial F}{\partial \boldsymbol{\sigma}'}, \qquad \mathbf{Q}' = \frac{\partial G}{\partial \boldsymbol{\sigma}'} \tag{15}$$

The positive scalar A' is defined as

$$A' = \mathbf{P}' : \mathbf{E}' : \mathbf{Q}' + H' > 0 \tag{16}$$

where H' is a generalized plastic modulus that is positive, zero or negative for hardening, perfect or softening plasticity, respectively.

Combining Eqs. (5), (9), (11) and (12), it has

$$\dot{\boldsymbol{\sigma}} = \mathbf{E} : \dot{\boldsymbol{\varepsilon}} \quad \text{elastic unloading} \tag{17}$$

$$\dot{\boldsymbol{\sigma}} = \mathbf{D} : \dot{\boldsymbol{\varepsilon}} \quad \text{plastic loading} \tag{18}$$

where the tangent stiffness moduli are given as

$$\mathbf{E} = \mathbf{E}' + K_F \boldsymbol{\delta} \otimes \boldsymbol{\delta} \tag{19}$$

$$\mathbf{D} = \mathbf{D}' + K_F \boldsymbol{\delta} \otimes \boldsymbol{\delta} \tag{20}$$

Eqs. (17) and (18) are the total stress–strain relations of the porous media under the undrained conditions.

3. Formulations of localization under undrained conditions

In the following derivations, we assume that the elastic–plastic porous media are isotropic and the inception of strain localization will be accompanied by the generation of a characteristic internal break surface (discontinuity) with unit normal **n**. The localization of deformation into shear bands takes place when a strain rate discontinuity occurs across the band. We assume that plastic loading is maintained for the primary as well as the bifurcated solutions. Upon using the conditions that the rate of total traction is continuous and that mass conservation prevails across the band, the following expressions can be derived from Eqs. (6) and (8) for porous media:

$$\mathbf{L}' \cdot \mathbf{m} + [\dot{P}_F^R]\mathbf{n} = 0 \tag{21}$$

$$\mathbf{m} \cdot \mathbf{n} - \frac{1}{K_F}[\dot{P}_F^R] = 0 \tag{22}$$

where **m** is a vector describing the discontinuity of the strain rate, $[\dot{P}_F^R]$ represents the discontinuity of the pore pressure rate, and $\mathbf{L}'$ is the effective characteristic tangent stiffness tensor (effective acoustic tensor), which is defined by

$$\mathbf{L}' = \mathbf{L}'^e - \frac{1}{A'}\mathbf{b} \otimes \mathbf{a}, \quad \mathbf{L}'^e = \mathbf{n} \cdot \mathbf{E}' \cdot \mathbf{n} \tag{23}$$

where the vectors **a** and **b** are defined as

$$\mathbf{a} = \mathbf{P}' : \mathbf{E}' \cdot \mathbf{n}, \qquad \mathbf{b} = \mathbf{Q}' : \mathbf{E}' \cdot \mathbf{n} \tag{24}$$

From Eqs. (21) and (22), we have

$$\mathbf{L} \cdot \mathbf{m} = 0 \tag{25}$$

where

$$\mathbf{L} = \mathbf{n} \cdot \mathbf{D} \cdot \mathbf{n} = \mathbf{L}' + K_F \mathbf{n} \otimes \mathbf{n} \tag{26}$$

Eliminating **m** between (21) and (22), we can also obtain

$$\left(\mathbf{n} \cdot \mathbf{M}' \cdot \mathbf{n} + \frac{1}{K_F} \right) [\dot{P}_F^R] = 0 \tag{27}$$

where tensor $\mathbf{M}'$ is the inverse of tensor $\mathbf{L}'$, which is derived as

$$\mathbf{M}' = (\mathbf{L}')^{-1} = \mathbf{M}'^e + \frac{1}{A' - \mathbf{a} : \mathbf{M}'^e : \mathbf{b}} (\mathbf{M}'^e \cdot \mathbf{b}) \otimes (\mathbf{a} \cdot \mathbf{M}'^e) \tag{28}$$

where $\mathbf{M}'^e = (\mathbf{L}'^e)^{-1}$. It is concluded that a non-trivial solution $[\dot{P}_F^R]$ of Eq. (27) is possible only if the scalar coefficient vanishes, i.e.

$$\mathbf{n} \cdot \mathbf{M}' \cdot \mathbf{n} + \frac{1}{K_F} = 0 \tag{29}$$

Combining Eqs. (16), (28) and (29), we obtain a condition on H' that must be satisfied at the onset of localization:

$$H' = -\mathbf{P}' : \mathbf{E}' : \mathbf{Q}' + \mathbf{a} \cdot \mathbf{M}'^e \cdot \mathbf{b} - \psi \frac{(\mathbf{a} \cdot \mathbf{M}'^e \cdot \mathbf{n})(\mathbf{b} \cdot \mathbf{M}'^e \cdot \mathbf{n})}{\mathbf{n} \cdot \mathbf{M}'^e \cdot \mathbf{n}} \tag{30}$$

where the scalar ψ is given as

$$\psi = \frac{K_F \mathbf{n} \cdot \mathbf{M}'^e \cdot \mathbf{n}}{1 + K_F \mathbf{n} \cdot \mathbf{M}'^e \cdot \mathbf{n}} \tag{31}$$

Following Ottosen and Runesson (1991), the critical-hardening modulus H'_{cr} corresponding to strain localization is defined as the constrained maximization of H' over all possible shear band directions **n** for a given state, i.e.

$$H'_{cr} = \mathrm{Max}\, H'(\mathbf{n}), \quad \text{s.t. } |\mathbf{n}| = 1 \tag{32}$$

Assuming that the solid phase is isotropic, then

$$\mathbf{E}_s = 2G \left(\mathbf{I} + \frac{v}{1 - 2v} \boldsymbol{\delta} \otimes \boldsymbol{\delta} \right) \tag{33}$$

where G is the shear modulus and v is Poisson's ratio of the solid phase. In general, $0 < v < 1/2$.

Inserting Eq. (33) into (13), we have

$$\mathbf{E}' = 2G(1 - m_F) \left[\mathbf{I} + \left(\frac{v}{1 - 2v} - \frac{K_F}{2G} \right) \boldsymbol{\delta} \otimes \boldsymbol{\delta} \right] \tag{34}$$

Substituting Eq. (34) into (23), it has

$$\mathbf{L}'^e = G(1 - m_F) \left[\left(\frac{1}{1 - 2v} - \frac{K_F}{G} \right) \mathbf{n} \otimes \mathbf{n} + \boldsymbol{\delta} \right] \tag{35}$$

$$\mathbf{M}'^{e} = \frac{1}{G(1-m_F)}\left[\frac{(1-2v)K_F - G}{G+(1-2v)(G-K_F)}\mathbf{n}\otimes\mathbf{n} + \boldsymbol{\delta}\right] \tag{36}$$

and the vectors **a** and **b** in Eq. (24) can be expressed as

$$\mathbf{a} = 2G(1-m_F)\left[\mathbf{P}'\cdot\mathbf{n} + \left(\frac{v}{1-2v} - \frac{K_F}{2G}\right)(\mathrm{tr}\,\mathbf{P}')\mathbf{n}\right] \tag{37}$$

$$\mathbf{b} = 2G(1-m_F)\left[\mathbf{Q}'\cdot\mathbf{n} + \left(\frac{v}{1-2v} - \frac{K_F}{2G}\right)(\mathrm{tr}\,\mathbf{Q}')\mathbf{n}\right] \tag{38}$$

By substituting Eqs. (34) and (36)–(38) into Eqs. (30) and (31), it has

$$\begin{aligned}\frac{H'}{2\widetilde{G}} = {} & 2\mathbf{n}\cdot(\mathbf{P}'\cdot\mathbf{Q}')\cdot\mathbf{n} + \frac{\tilde{v}(1-\psi)}{1-\tilde{v}}[(\mathbf{n}\cdot\mathbf{Q}'\cdot\mathbf{n})\,\mathrm{tr}\,\mathbf{P}' + (\mathbf{n}\cdot\mathbf{P}'\cdot\mathbf{n})\,\mathrm{tr}\,\mathbf{Q}'] \\ & - \frac{1+(1-2\tilde{v})\psi}{1-\tilde{v}}(\mathbf{n}\cdot\mathbf{P}'\cdot\mathbf{n})(\mathbf{n}\cdot\mathbf{Q}'\cdot\mathbf{n}) - \frac{\tilde{v}(1-2\tilde{v})+\tilde{v}^2\psi}{(1-\tilde{v})(1-2\tilde{v})}(\mathrm{tr}\,\mathbf{P}')(\mathrm{tr}\,\mathbf{Q}') - \mathbf{P}':\mathbf{Q}'\end{aligned} \tag{39}$$

where

$$\psi = \left(\frac{1-2\tilde{v}}{1-\tilde{v}}\frac{K_F}{2\widetilde{G}}\right)\left(1+\frac{1-2\tilde{v}}{1-\tilde{v}}\frac{K_F}{2\widetilde{G}}\right)^{-1} \tag{40}$$

$$\widetilde{G} = (1-m_F)G \tag{41}$$

$$\tilde{v} = \frac{2vG-(1-2v)K_F}{2[G-(1-2v)K_F]} \tag{42}$$

When the porosity $m_F = 0$, the porous material reduces to a single-phase solid material, i.e., $K_F = 0$, $\psi = 0$. As a result, the solution of the porous media expressed by Eq. (39) reduces to the solution of the single-phase solid obtained by Ottosen and Runesson (1991).

When the porosity $m_F \neq 0$ and the saturation $m_L = 0$, the porous media are mixtures made up of a solid and a gas, namely $K_F = K_G$. With the increment of the gas compressibility, $K_F = K_G \to 0$, and then $\psi \to 0$, $\tilde{v} \to v$. When the porous media are fully saturated, as liquid has little compressibility, $K_F = K_L \to \infty$, which causes $\psi \to 1/m_F$, $\tilde{v} \to 1/2$. Thus, for the porous media in geotechnical engineering, the parameter ψ can reflect the degree of saturation of the porous media indirectly, and $0 < \psi < 1/m_F$. For soils the ratio $K_F/2G$ generally ranges from 10^{-1} to 10^3, which represents the extreme states of moduli for partial and full liquid saturation, respectively. Choosing $v = 0.2$, which is typical for clay, and assuming $m_F = 0.4$, then ψ ranges from 0.12 to 2.5. In addition, it should be noted that the parameter $\tilde{v}$ ranges from $-\infty$ to $+\infty$ with the variation of ratio $K_F/2G$ when Poisson's ratio v remains constant.

4. Critical hardening modulus and the corresponding direction of shear band initiation under plane strain condition

It is assumed that $\mathbf{P}'$ and $\mathbf{Q}'$ possess the same principal directions and two of the principal directions (x_1 and x_2) are located in the plane of interest. Hence, the x_3-direction is out of plane and $n_3 = 0$. Without loss of generality we also label the in-plane axes so that $P'_1 \geqslant P'_2$. Under very mild constraints on the flow rule, this choice will also imply that $Q'_1 \geqslant Q'_2$, which is assumed subsequently.

With the assumption given above, the expression for H' at strain localization in plane strain can be expressed as a special case of Eq. (39), i.e.

$$\frac{H'}{2\widetilde{G}} = a_1 n_1^2 + a_2 n_2^2 - \frac{1+(1-2\tilde{v})\psi}{1-\tilde{v}}\left(P_1' n_1^2 + P_2' n_2^2\right)\left(Q_1' n_1^2 + Q_2' n_2^2\right) - k \tag{43}$$

where

$$a_\alpha = 2P_\alpha' Q_\alpha' + \frac{\tilde{v}(1-\psi)}{1-\tilde{v}}(Q_\alpha' \operatorname{tr}\mathbf{P}' + P_\alpha' \operatorname{tr}\mathbf{Q}'), \quad \alpha = 1,2 \text{ (no summation)} \tag{44}$$

and

$$k = \frac{\tilde{v}(1-2\tilde{v}) + \tilde{v}^2\psi}{(1-\tilde{v})(1-2\tilde{v})}(\operatorname{tr}\mathbf{P}')(\operatorname{tr}\mathbf{Q}') + P_1'Q_1' + P_2'Q_2' + P_3'Q_3' \tag{45}$$

In order to get the critical value H'_{cr} corresponding to initiation of shear banding, we differentiate Eq. (43)

$$\frac{d}{d(n_1^2)}\left(\frac{H'}{2\widetilde{G}}\right) = \frac{1}{1-\tilde{v}}\left[c_1 - (c_1 - c_2)n_1^2\right] = 0 \tag{46}$$

where c_1 and c_2 are given as

$$c_1 = (P_1' - P_2')(Q_1' + \tilde{v}Q_3') + (Q_1' - Q_2')(P_1' + \tilde{v}P_3') - \psi r_1 \tag{47}$$

$$c_2 = (P_1' - P_2')(Q_2' + \tilde{v}Q_3') + (Q_1' - Q_2')(P_2' + \tilde{v}P_3') - \psi r_2 \tag{48}$$

and r_1 and r_2 are given as

$$r_1 = (P_1' - P_2')[\tilde{v}\operatorname{tr}\mathbf{Q}' + (1-2\tilde{v})Q_2'] + (Q_1' - Q_2')[\tilde{v}\operatorname{tr}\mathbf{P}' + (1-2\tilde{v})P_2'] \tag{49}$$

$$r_2 = (P_1' - P_2')[\tilde{v}\operatorname{tr}\mathbf{Q}' + (1-2\tilde{v})Q_1'] + (Q_1' - Q_2')[\tilde{v}\operatorname{tr}\mathbf{P}' + (1-2\tilde{v})P_1'] \tag{50}$$

If

$$\frac{d^2}{d(n_1^2)^2}\left(\frac{H'}{2\widetilde{G}}\right) = -\frac{1}{1-\tilde{v}}(c_1 - c_2) < 0 \tag{51}$$

is satisfied, then the solutions of Eq. (46) which satisfy $0 \leqslant n_1^2 \leqslant 1$ correspond to the maximum value of H'.

Only the case defined by $P_1' > P_2'$, $Q_1' > Q_2'$ will be discussed hereafter. From Eq. (46), it has

$$n_1^2 = \frac{c_1}{c_1 - c_2}, \qquad n_2^2 = 1 - n_1^2 = -\frac{c_2}{c_1 - c_2} \tag{52}$$

which is valid whenever $0 \leqslant n_1^2 \leqslant 1$ (or $1 \geqslant n_2^2 \geqslant 0$) is satisfied, then the directions of shear band initiation can be defined as

$$\tan^2\theta = \frac{n_1^2}{n_2^2} = -\frac{c_1}{c_2} \tag{53}$$

where θ denotes the angle in the x_1, x_2-plane between the x_2-axis and the normal vector (n_1, n_2), and it is assumed that $0° \leqslant \theta \leqslant 90°$. The corresponding maximum hardening modulus H'_{cr} can be obtained by inserting Eq. (52) into Eq. (43).

If the condition $0 \leqslant n_1^2 \leqslant 1$ is not satisfied, the following cases occur:

- When $\frac{d}{d(n_1^2)}\left(\frac{H'}{2\widetilde{G}}\right) < 0$, H' assumes its maximum value when $\theta = 0°$.
- Similarly, when $\frac{d}{d(n_1^2)}\left(\frac{H'}{2\widetilde{G}}\right) > 0$, H' assumes its maximum value at $\theta = 90°$.

5. Analysis of strain localization based on the Mohr–Coulomb criterion

The Mohr–Coulomb yield criterion and plastic potential can be defined as follows:

$$F = \tfrac{1}{2}(\sigma'_{\mathrm{I}} - \sigma'_{\mathrm{III}}) + \tfrac{1}{2}(\sigma'_{\mathrm{I}} + \sigma'_{\mathrm{III}}) \sin\varphi - c = 0 \tag{54}$$

$$G = \tfrac{1}{2}(\sigma'_{\mathrm{I}} - \sigma'_{\mathrm{III}}) + \tfrac{1}{2}(\sigma'_{\mathrm{I}} + \sigma'_{\mathrm{III}}) \sin\varphi^* \tag{55}$$

where $\sigma'_{\mathrm{I}} \geqslant \sigma'_{\mathrm{II}} \geqslant \sigma'_{\mathrm{III}}$ are the effective principal stresses (which are taken positive in compression), φ is the angle of internal friction, φ^* is the angle of dilatancy, and c is a cohesion intercept. It should be noted that generally $\varphi \geqslant \varphi^* \geqslant 0$.

Since the in-plane effective principal stresses are usually defined as $\sigma'_1 \geqslant \sigma'_2$, there are three cases depending on the magnitude of the out-of-plane stress σ'_3.

Case A. When $\sigma'_1 \geqslant \sigma'_2 \geqslant \sigma'_3$, it has $\sigma'_{\mathrm{I}} = \sigma'_1$ and $\sigma_{\mathrm{III}} = \sigma'_3$, and from Eqs. (54) and (55),

$$P'_1 = \tfrac{1}{2}(1 + \sin\varphi), \qquad P'_2 = 0, \qquad P'_3 = -\tfrac{1}{2}(1 - \sin\varphi) \tag{56}$$

$$Q'_1 = \tfrac{1}{2}(1 + \sin\varphi^*), \qquad Q'_2 = 0, \qquad Q'_3 = -\tfrac{1}{2}(1 - \sin\varphi^*) \tag{57}$$

and

$$\mathrm{tr}\,\mathbf{P}' = \sin\varphi, \qquad \mathrm{tr}\,\mathbf{Q}' = \sin\varphi^* \tag{58}$$

Substituting Eqs. (56)–(58) into Eqs. (47) and (48), it has

$$c_1 = \frac{1}{2}A_1 - \frac{\tilde{v}\psi}{2}A_2, \qquad c_2 = -\frac{\tilde{v}}{2}A_3 - \frac{\psi}{2}A_4 \tag{59}$$

where

$$A_1 = 1 - \tilde{v} + \sin\varphi + \sin\varphi^* + (1 + \tilde{v}) \sin\varphi \sin\varphi^*$$

$$A_2 = \sin\varphi + \sin\varphi^* + 2 \sin\varphi \sin\varphi^*$$

$$A_3 = 1 - \sin\varphi \sin\varphi^*$$

$$A_4 = 1 - 2\tilde{v} + (1 - \tilde{v})(\sin\varphi + \sin\varphi^*) + \sin\varphi \sin\varphi^*$$

If the condition defined by Eq. (51) is satisfied, from Eqs. (52) and (53), the following can be derived

$$n_1^2 = \frac{A_1 - \tilde{v}\psi A_2}{A_1 - \tilde{v}\psi A_2 + \tilde{v}A_3 + \psi A_4}, \qquad n_2^2 = \frac{\tilde{v}A_3 + \psi A_4}{A_1 - \tilde{v}\psi A_2 + \tilde{v}A_3 + \psi A_4} \tag{60}$$

$$\tan^2\theta = \frac{A_1 - \tilde{v}\psi A_2}{\tilde{v}A_3 + \psi A_4} \tag{61}$$

which is valid whenever $0 \leqslant n_1^2 \leqslant 1$. The corresponding maximum hardening modulus can be obtained by substituting Eq. (60) into (43).

Case B. When $\sigma'_1 \geqslant \sigma'_3 \geqslant \sigma'_2$, it has $\sigma'_{\mathrm{I}} = \sigma'_1$ and $\sigma'_{\mathrm{III}} = \sigma'_2$, and from Eqs. (54) and (55),

$$P'_1 = \tfrac{1}{2}(1 + \sin\varphi), \qquad P'_2 = -\tfrac{1}{2}(1 - \sin\varphi), \qquad P'_3 = 0 \tag{62}$$

$$Q'_1 = \tfrac{1}{2}(1 + \sin\varphi^*), \qquad Q'_2 = -\tfrac{1}{2}(1 - \sin\varphi^*), \qquad Q'_3 = 0 \tag{63}$$

and

$$\mathrm{tr}\,\mathbf{P}' = \sin\varphi, \qquad \mathrm{tr}\,\mathbf{Q}' = \sin\varphi^* \tag{64}$$

Then c_1 and c_2 can be similarly derived and given as

$$c_1 = \frac{1}{2}B_1 - \frac{\psi}{2}B_2, \qquad c_2 = -\frac{1}{2}B_3 + \frac{\psi}{2}B_4 \tag{65}$$

where

$$B_1 = 2 + \sin\varphi + \sin\varphi^*$$

$$B_2 = 4\tilde{v} - 2 + \sin\varphi + \sin\varphi^*$$

$$B_3 = 2 - \sin\varphi - \sin\varphi^*$$

$$B_4 = 4\tilde{v} - 2 - \sin\varphi - \sin\varphi^*$$

If the condition defined by Eq. (51) is satisfied, then

$$n_1^2 = \frac{B_1 - \psi B_2}{B_1 - \psi B_2 + B_3 - \psi B_4}, \qquad n_2^2 = \frac{B_3 - \psi B_4}{B_1 - \psi B_2 + B_3 - \psi B_4} \tag{66}$$

$$\tan^2\theta = \frac{B_1 - \psi B_2}{B_3 - \psi B_4} \tag{67}$$

which is valid whenever $0 \leqslant n_1^2 \leqslant 1$. The corresponding maximum hardening modulus can be obtained by substituting Eq. (66) into (43).

Case C. If $\sigma_3' \geqslant \sigma_1' \geqslant \sigma_2'$, then $\sigma_{\mathrm{I}}' = \sigma_3'$, $\sigma_{\mathrm{III}}' = \sigma_2'$, and from Eqs. (54) and (55), it has

$$P_1' = 0, \qquad P_2' = -\tfrac{1}{2}(1 - \sin\varphi), \qquad P_3' = \tfrac{1}{2}(1 + \sin\varphi) \tag{68}$$

$$Q_1' = 0, \qquad Q_2' = -\tfrac{1}{2}(1 - \sin\varphi^*), \qquad Q_3' = \tfrac{1}{2}(1 + \sin\varphi^*) \tag{69}$$

where

$$\mathrm{tr}\,\mathbf{P}' = \sin\varphi, \qquad \mathrm{tr}\,\mathbf{Q}' = \sin\varphi^* \tag{70}$$

Similarly, it has

$$c_1 = \frac{\tilde{v}}{2}C_1 - \frac{\psi}{2}C_2, \qquad c_2 = \frac{1}{2}C_3 - \frac{\tilde{v}\psi}{2}C_4 \tag{71}$$

where

$$C_1 = 1 - \sin\varphi\sin\varphi^*$$

$$C_2 = 2\tilde{v} - 1 + (1 - \tilde{v})(\sin\varphi + \sin\varphi^*) - \sin\varphi\sin\varphi^*$$

$$C_3 = \tilde{v} - 1 + \sin\varphi + \sin\varphi^* - (1 + \tilde{v})\sin\varphi\sin\varphi^*$$

$$C_4 = \sin\varphi + \sin\varphi^* - 2\sin\varphi\sin\varphi^*$$

If the condition defined by Eq. (51) holds, then

$$n_1^2 = \frac{\tilde{v}C_1 - \psi C_2}{\tilde{v}C_1 - \psi C_2 - C_3 + \tilde{v}\psi C_4}, \qquad n_2^2 = \frac{-C_3 + \tilde{v}\psi C_4}{\tilde{v}C_1 - \psi C_2 - C_3 + \tilde{v}\psi C_4} \tag{72}$$

$$\tan^2\theta = \frac{\tilde{v}C_1 - \psi C_2}{-C_3 + \tilde{v}\psi C_4} \tag{73}$$

which is valid whenever $0 \leqslant n_1^2 \leqslant 1$. The corresponding maximum hardening modulus can be similarly determined by substituting Eq. (72) into (43).

6. Comparison with the experimental results

The behavior of water-saturated granular materials subjected to undrained deformations under plane strain condition has been investigated by Han and Vardoulakis (1991). The experimental results about the shear band orientations Θ presented in that study indicate a relation $\Theta = 90° - \theta$. When the porous media are fully saturated, by assuming the liquid is completely incompressible, from Eqs. (40) and (42), it has $\psi = 1/m_F$, and $\tilde{v} = 0.5$. Hence it can be concluded that the properties of strain localization of fully saturated porous media under undrained conditions are independent of Poisson's ratio if assuming the liquid is totally incompressible.

Although the liquid in fully saturated porous media has little compressibility, it is in fact not completely incompressible. Here we let $K_F/2G = 1000$ correspond to the fully saturated state, then from Eq. (42) it has

$$\tilde{v} = \frac{2001v - 1000}{4000v - 1999} \tag{74}$$

It is noted from Eq. (74) that the values of $\tilde{v}$ are approximately equal to 0.50025 when Poisson's ratio v ranges from 0.01 to 0.49. Hence it can be regarded that the properties of strain localization of fully saturated porous media under undrained conditions are almost independent of Poisson's ratio.

For the plane strain problems in practical engineering, the out-of-plane principal stress is usually the intermediate principal stress (Lee and Ghosh, 1996), and the stress state is the same as that of case B in Section 5. If the deformation inside the shear band is undrained and the band material is fully saturated, the shear band dilatancy angle φ^* must be zero (Han and Vardoulakis, 1991). Table 1 shows the comparison of the experiment results and the solutions with the present method in this paper (based on the Mohr–Coulomb yield criterion).

It is observed from Table 1 that the solution derived by the present method which considers the influence of the porosity on the properties of shear banding are in good agreement with the experimental results.

7. Examples

In this section, based on the Mohr–Coulomb criterion, the influences of some material parameters on the properties of the strain localization for the plane strain problems are discussed. As the out-of-plane principal stress is usually the intermediate principal stress for the plane strain problems in practical engineering, only the stress state of case B in Section 5 is considered.

Table 1
Comparison of shear band directions

Test	m_F	φ	φ^*	Θ (experiment)	$\Theta = 90° - \theta$ (present theory)
DC4	0.393	≈33°	0°	57°	57.4°
DC11	0.374	≈32°	0°	60°	58.2°
LC3	0.371	≈29°	0°	60°	57.2°
LC4	0.410	≈17°	0°	56°	51.3°
DC17	0.407	≈30°	0°	55°	55.7°

When $K_F/G = 1$, the porous media are in the case of partial saturation. The dependence of the initiation direction of the shear band and the corresponding maximum hardening modulus on the porosity is shown in Figs. 1 and 2, which is for the particular choice $\varphi = 25°$ and $\varphi^* = 5°$ and for different values of Poisson's ratio v. It can be observed from Fig. 1 that the direction θ of the shear band initiation decreases with the increase of the porosity m_F for all the three cases with $v = 0.2$, $v = 0.3$ and $v = 0.4$. It also shows that at the same porosity, the angle θ of the shear band initiation is larger when Poisson's ratio is larger. It is shown from Fig. 2 that the effect of porosity on the hardening modulus is much dependent on Poisson's ratio. When the porosity remains constant, the hardening modulus decreases with the increase of Poisson's ratio.

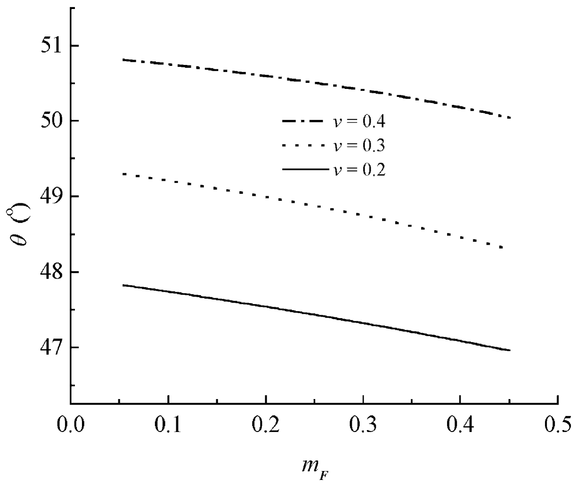

Fig. 1. Variation of the shear band direction with the porosity for $\varphi = 25°$, $\varphi^* = 5°$ in the case $\sigma'_1 \geqslant \sigma'_3 \geqslant \sigma'_2$ based on the Mohr–Coulomb yield criterion for partially saturated porous media.

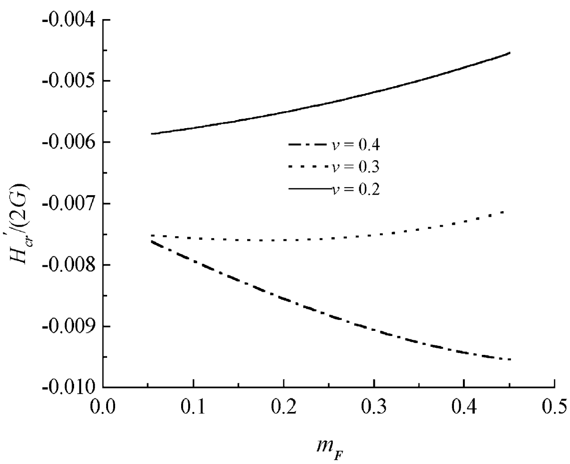

Fig. 2. Variation of the maximum hardening modulus with the porosity for $\varphi = 25°$, $\varphi^* = 5°$ in the case $\sigma'_1 \geqslant \sigma'_3 \geqslant \sigma'_2$ based on the Mohr–Coulomb yield criterion for partially saturated porous media.

When $K_F/2G = 1000$, the porous media can be regarded as fully saturated. The effect of the porosity on the initiation direction of the shear band and the corresponding maximum hardening modulus is respectively shown in Figs. 3 and 4 for the case of $\varphi = 25°$ and $\varphi^* = 5°$. It is obvious from Figs. 3 and 4 that the porosity of the porous media significantly influences the initiation direction of the shear band and the corresponding maximum hardening modulus. Thus it is of great importance to take account of the porosity in the analysis of the strain localization properties of porous media. Furthermore, for fully saturated porous media with $\varphi = 25°$ and $m_F = 0.4$, variation of the direction of the shear band initiation and the corresponding maximum hardening modulus with the angle of dilatancy that ranges from 0° to 25° is estimated and shown in Figs. 5 and 6, respectively. It is observed that the angle θ of the shear band initiation decreases almost linearly with the increase of the dilatancy angle while the corresponding hardening modulus increases almost linearly with the increase of the dilatancy angle.

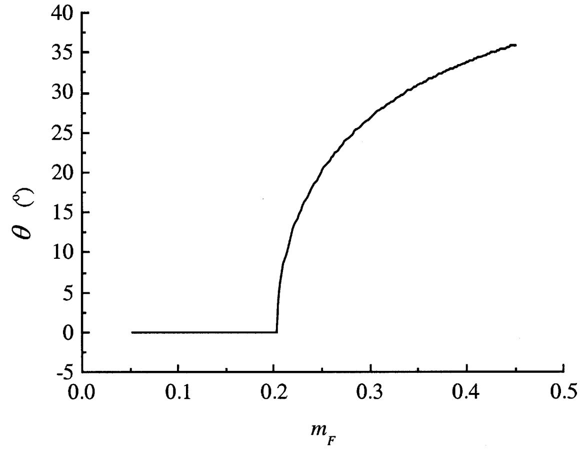

Fig. 3. Variation of the shear band direction with the porosity for $\varphi = 25°$, $\varphi^* = 5°$ in the case $\sigma'_1 \geqslant \sigma'_3 \geqslant \sigma'_2$ based on the Mohr–Coulomb yield criterion for fully saturated porous media.

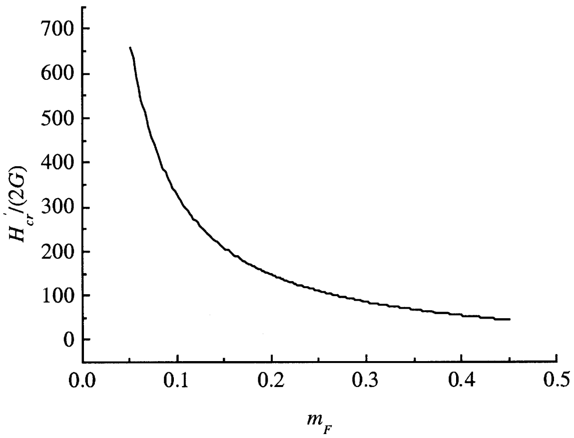

Fig. 4. Variation of the maximum hardening modulus with the porosity for $\varphi = 25°$, $\varphi^* = 5°$ in the case $\sigma'_1 \geqslant \sigma'_3 \geqslant \sigma'_2$ based on the Mohr–Coulomb yield criterion for fully saturated porous media.

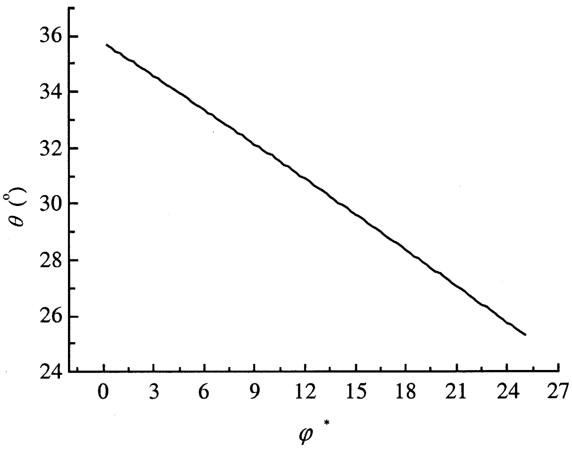

Fig. 5. Variation of the shear band direction with the dilatancy angle for $\varphi = 25°$ and $m_F = 0.4$ in the case $\sigma_1' \geqslant \sigma_3' \geqslant \sigma_2'$ based on the Mohr–Coulomb yield criterion for fully saturated porous media.

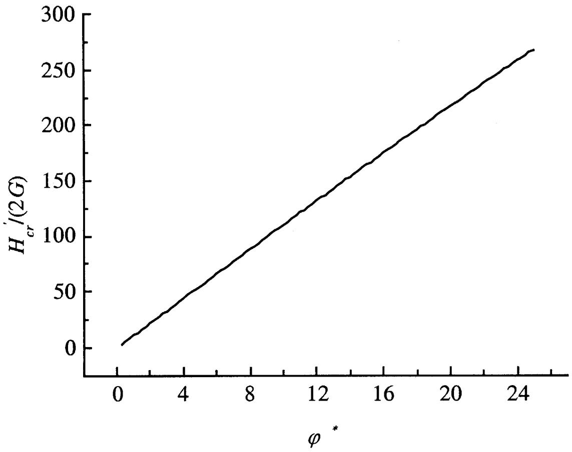

Fig. 6. Variation of the maximum hardening modulus with the dilatancy angle for $\varphi = 25°$ and $m_F = 0.4$ in the case $\sigma_1' \geqslant \sigma_3' \geqslant \sigma_2'$ based on the Mohr–Coulomb yield criterion for fully saturated porous media.

Finally, the influence of degree of saturation on the properties of strain localization is investigated. As it ranges from 0 to $1/m_F$ when the ratio $K_F/2G$ varies from 0 to ∞, the parameter ψ indicates indirectly the degree of saturation of the porous media. The relation between the direction θ of shear band initiation and the parameter ψ is shown in Fig. 7 while that between the corresponding hardening modulus H_{cr}' and the parameter ψ is shown in Fig. 8, both for the case of $\varphi = 25°$, $\varphi^* = 5°$, $m_F = 0.4$ and $v = 0.2$. It is shown that the angle θ of shear band initiation decreases with the increase of the degree of saturation. However, the hardening modulus decreases slightly with the increase of the degree of saturation when the degree of saturation is low, and increases sharply with the increase of the degree of saturation when the degree of saturation is high.

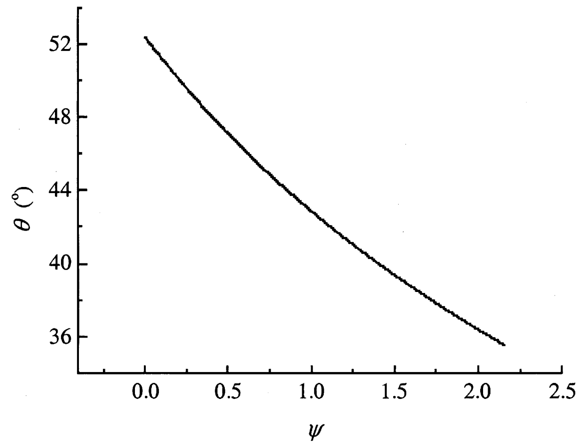

Fig. 7. Variation of the shear band direction θ with ψ for $\varphi = 25°$, $\varphi^* = 5°$, $m_F = 0.4$ and $\nu = 0.2$ in the case $\sigma_1' \geqslant \sigma_3' \geqslant \sigma_2'$ for based on the Mohr–Coulomb yield criterion.

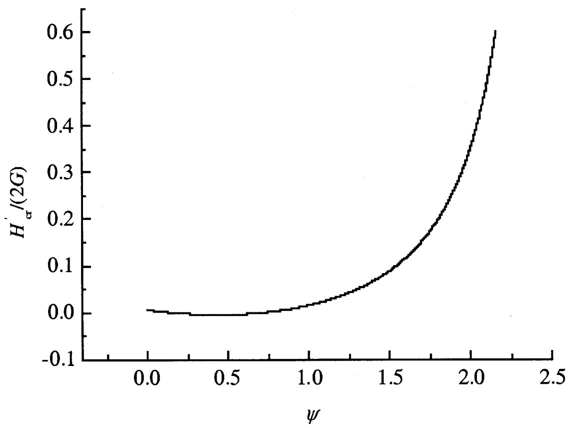

Fig. 8. Variation of the maximum hardening modulus H'_{cr} with ψ for $\varphi = 25°$, $\varphi^* = 5°$, $m_F = 0.4$ and $\nu = 0.2$ in the case $\sigma_1' \geqslant \sigma_3' \geqslant \sigma_2'$ based on the Mohr–Coulomb yield criterion.

8. Conclusions

Within the general framework of mixture theory, the effective stress–strain and total stress–strain relations of the three-phase elastic–plastic porous media under undrained conditions are derived. Based on the obtained elastic–plastic constitutive equations and by introducing the fictitious "fluid phase" as a mixture of liquid and gas, the conditions for localization of deformation into a shear band in the incremental response of partially saturated and fully saturated porous media under undrained conditions are determined, in which the effect of porosity on the strain localization is included.

The explicit analytical expressions of the direction of shear band initiation and the corresponding hardening modulus of the porous media for the plane strain case are deduced. With reference to Mohr–Coulomb yield criterion, an analysis of the influence of the porosity on the properties of strain localization is performed. The results indicate that the properties of strain localization are much dependent on the porosity, and the relation between the shear band property of partially saturated porous media and the porosity depends on Poisson's ratio v. However, the properties of strain localization for the fully saturated porous media are almost independent of Poisson's ratio. If assuming the liquid is totally incompressible, the strain localization of fully saturated porous media under undrained conditions is completely independent of Poisson's ratio.

Parametric investigation of the influences of the degree of saturation and the angle of dilatancy on the properties of strain localization indicates that both the degree of saturation and the angle of dilatancy are of great importance in the analysis of strain localization for the porous media. On the basis of Mohr–Coulomb yield criterion, use is made of the theory presented in this paper to obtain the solutions of the shear banding orientation, which are proved to be in good agreement with the experimental results.

References

Bigoni, D., Hueckel, T., 1991a. Uniqueness and localization—I. Associative and non-associative elastoplasticity. Int. J. Solids Struct. 28, 197–214.

Bigoni, D., Hueckel, T., 1991b. Uniqueness and localization—II. Coupled elastoplasticity. Int. J. Solids Struct. 28, 215–224.

Bowen, R.M., 1982. Compressible porous media models by use of the theory of mixtures. Int. J. Eng. Sci. 20, 697–735.

Hadamard, J., 1903. Leçons sur la propagation des ondes et les equations de l'hydrodynamique. In: Librairie Scientifique A. Hermann, Paris, France.

Han, C., Vardoulakis, I., 1991. Plane strain compression experiments on water-saturated fine-grained sand. Geotechnique 41, 49–78.

Hill, R., 1962. Acceleration waves in solids. J. Mech. Phys. Solids 10, 1–16.

Lee, Y.K., Ghosh, J., 1996. Significance of J_3 to the prediction of shear bands. Int. J. Plasticity 12, 1179–1197.

Mandel, J., 1963. Propagation des surfaces de discontinuite dans un milieu elasto-plastique. In: Kolsky, H., Prager, W. (Eds.), Proceedings of the IUTAM Symposium on Stress Waves in Inelastic Solids. Springer-Verlag, Berlin, pp. 337–344.

Molenkamp, F., 1985. Comparison of frictional material models with respect to shear band initiation. Geotechnique 35, 127–143.

Ottosen, N.S., Runesson, K., 1991. Properties of discontinuous bifurcation solutions in elasto-plasticity. Int. J. Solids Struct. 27, 401–421.

Read, H.E., Hegemier, G.A., 1984. Strain softening of rock, soil and concrete—A review article. Mech. Mat. 3, 271–294.

Rice, J.R., 1975. On the stability of dilatant hardening for saturated rock masses. J. Geophys. Res. 80, 1531–1536.

Rice, J.R., 1976. The localization of plastic deformation. In: Koiter, W.T. (Ed.), Proceedings of the 14th IUTAM Congress: Theoretical and Applied Mechanics. North-Holland, Amsterdam, pp. 207–220.

Rice, J.R., Cleary, M.P., 1976. Some basic stress diffusion solutions for fluid-saturated elastic porous media with compressible contents. Rev. Geophys. Space Phys. 14, 227–241.

Rice, J., Rudnicki, J.W., 1980. A note on some features on the theory of localization of deformation. Int. J. Solids Struct. 16, 597–605.

Rudnicki, J.W., 1983. A formulation for studying coupled deformation pore fluid diffusion effects on localization of deformation. In: Nemat-Nasser, S. (Ed.), Geomechanics, AMD-vol. 57. ASME, pp. 35–44.

Rudnicki, J., Rice, J., 1975. Conditions for the localization of deformation in sensitive dilatant materials. J. Mech. Phys. Solids 23, 371–394.

Runesson, K., Ottosen, N.S., Peric, D., 1991. Discontinuous bifurcations of elastic–plastic solutions at plane stress and plane strain. Int. J. Plasticity 7, 99–121.

Runesson, K., Peric, D., Sture, S., 1996. Effect of pore fluid compressibility on localization in elastic–plastic porous solids under undrained conditions. Int. J. Solids Struct. 33, 1501–1518.

Schreyer, H.L., Zhou, S., 1995. A unified approach for predicting material failure and decohesion. In: Geomechanics, AMD-vol. 200/MD-vol. 57. ASME, New York, pp. 203–214.

Terzaghi, K., 1943. Theoretical Soil Mechanics. John Wiley and Sons, New York.

Thomas, T.Y., 1961. Plastic Flow and Fracture in Solids. Academic Press, New York.

Vardoulakis, I., 1980. Shear band inclination and shear modulus of sand in biaxial tests. Int. J. Numer. Anal. Meth. Geomech. 4, 103–119.

Yang, S.Y., Yu, M.H., 2000. Constitutive model of multi-phase porous media. Acta Mechanica Sinica 32, 11–24 (in Chinese).

Zhang, H.W., Schrefler, B.A., 2001. Uniqueness and localization analysis of elastic–plastic saturated porous media. Int. J. Numer. Anal. Meth. Geomech. 25, 29–48.

Zienkiewicz, O.C. et al., 1993. A new algorithm for coupled soil–pore fluid problem. Shock and Vibration 1, 3–13.

Życzkowski, M., 1999. Discontinuous bifurcations in the case of the Burzyński–Torre yield condition. Acta Mechanica 132, 19–35.